ELSEVIER

Cement and Concrete Composites **19** (1997) 241–257

0958-9465/97/$17.00

PII:S0958-9465(97)00014-0

The Collapse Mechanism of a Subway Station during the Great Hanshin Earthquake

Xuehui An,[a] Ashraf A. Shawky[b] & Koichi Maekawa[a]

[a]Department of Civil Engineering, University of Tokyo (Hongo 7-3-1, Bunkyo-ku, Tokyo, 113 Japan
[b]Department of Structural Engineering, Cairo University, Giza, Egypt

Abstract

The Great Hanshin earthquake, on 17 January 1995, brought about serious damage to some underground reinforced concrete (RC) structures serving the subway in Kobe city, Japan. In this study, the seismic response of Daikai subway station during this earthquake is computed by FEM code WCOMD-SJ, which is a two-dimensional dynamic finite element program including path dependent RC smeared model, soil foundation model and interfacial model. The shear failure of intermediate column of the station can be reasonably simulated and it is concluded that the failure of the intermediate column is caused by low shear capacity and poor ductility. Enhancement of seismic resistance is also discussed using this FEM code. © *1997 Elsevier Science Ltd. All rights reserved.*

INTRODUCTION

In the history of earthquakes, reinforced concrete (RC) underground structures have had some soundness, though some cracks were induced during an earthquake, but no complete collapse of an RC underground structure was recorded. Many structural engineers believed that RC underground structures might not be seriously damaged during earthquakes, until the Great Hanshin earthquake. The Great Hanshin earthquake, on 17 January 1995, brought about catastrophic damage and collapse to some of the RC underground structures serving the subway in Kobe city. At the same time, many other underground structures survived and exhibited soundness with different levels. It is a duty of structural engineers to clarify the chief causes of collapse of RC underground structures.

First, this paper summarizes serious damage and collapse of RC underground structures and, second, presents analytical results of the nonlinear dynamic responses for discussing the mechanism of the collapse of underground structures. In this study, two cases will be discussed. One is the underground subway station that failed seriously. The other is the tunnel section that was safe and connected to the collapsed station. Through these investigations, the authors aim to learn some engineering lessons for the future seismic resistant design of RC underground structures.

FAILURE OF UNDERGROUND SUBWAY STATION

Along the Kobe subway line, a lot of damage was caused to the underground structures.[1,2] For all the different sections along the line, the underground structure is composed of RC frames having an intermediate column with a rectangular section. In almost all sections, diagonal shear cracks were clearly observed, as shown in Fig. 1(a). In some sections, few diagonal shear cracks in the column are observed. For another section, the diagonal shear cracks were associated with the splitting of concrete volume, but still the column has a load-carrying mechanism against the vertical loads (see Fig. 1(a)).

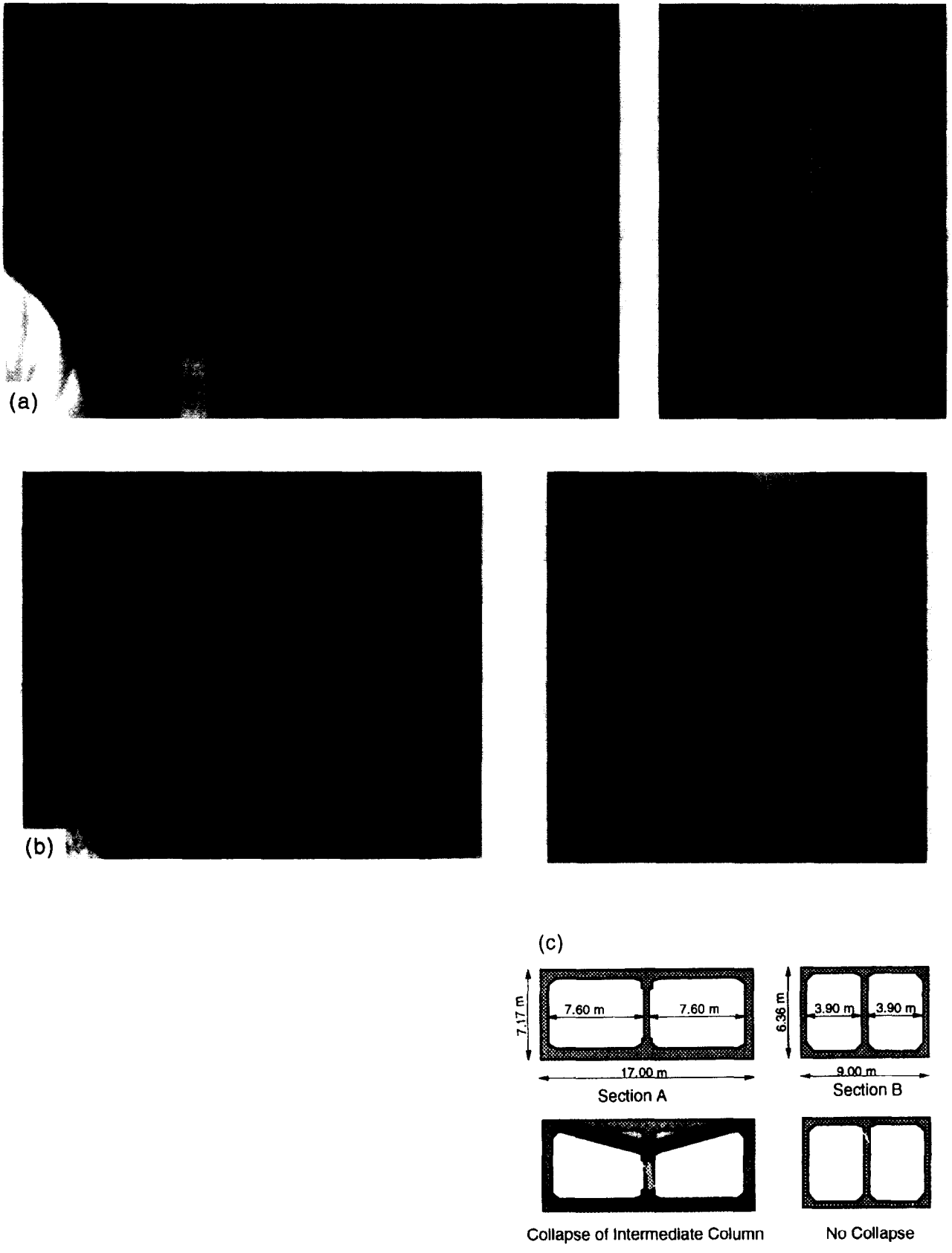

Fig. 1. (a) Shear cracks found in intermediate columns. (b) Collapse of RC underground structure. (c) Different sections for RC structures.

As for the completely damaged sections, the columns with diagonal shear crack loose load-carrying mechanism against the vertical forces were associated with dead loads applied on the top slab and soil overlayer. As a result, the top slab was completely collapsed, as shown in Fig. 1(b).

As in extreme cases, two sections will be analyzed to identify the failure mechanism in use of the numerical analysis. Figure 1(c) shows two different sections which are used in this study. Section A is one of the sections of the station which has complete collapse of the intermediate column. The other section, which is on the tunnel line between two stations, has few diagonal shear cracks (section B). The distance between both sections is less than 10 m. As a matter of fact, section A was completely damaged and section B underwent very few cracks. The same earthquake action is supposed to be applied to both sections. Then, it is crucial to clarify the seismic resistant performance of both structures for identifying the collapse mechanism.

ANALYTICAL DISCUSSION FOR UNDERGROUND SUBWAY STATION

The authors focus on the collapse mechanism of the RC underground structure, especially the intermediate column, in the analysis. The ground motion was not obtained at the site of the structures. Thus, three different earthquake waves, which were actually measured at Kobe meteorological observatory, Higashi–Kobe bridge and Amagasaki city close to the structure concerned, were used for the dynamic analysis. One of the characteristics of the seismic load in Kobe is its higher level of up–down component of the ground motion. At the same time, the ratio between horizontal component and up–down component is drastically changed. The first record (see Fig. 2) shows a very high horizontal ground acceleration with short period. The maximum vertical acceleration is about 40% of the maximum horizontal one. The second one (see Fig. 2) exhibits the great up–down acceleration component compared with the horizontal one (140% of the maximum horizontal component). The third record (see Fig. 2) shows a medium acceleration level for both acceleration components with long period. The maximum acceleration in both directions (horizontal and up–down) is almost equal.

Computational tool

Nonlinear dynamic finite element analysis code named WCOMD-SJ[3] was applied for investigation of the collapse mechanism. Constitutive models for reinforced concrete, soil and interface between soil and RC, respectively, are installed.

For the constitutive model of reinforced concrete, the combination of smeared and discrete crack models, subjected to reversed cyclic loads,[4] is adopted. A smeared crack model is employed for in-plane elements based on a multi-directional fixed smeared crack approach[4] and discrete ones are placed in between members with different thickness, construction joints and fewer discrete cracks intersecting reinforcement. Since both smeared and discrete cracks have distinct size sensitivity to energy dissipation,[5] their combination is crucial for computing ductility and energy absorption of scaled-up structures in seismic analysis. These models were verified under reversed cyclic loading paths of wide variety (Fig. 3).

A path-dependent constitutive model for soil is indispensable for dealing with kinematic interaction of RC/soil entire system under strong seismic loads.[7] Here, Ohasaki's model[8] defines the formula for envelope to express the nonlinear relation of the shear stress–strain for soil as well as internal loop with Masing's rule (Fig. 3). In addition, separation and sliding between the soil and the RC structure are taken into account along the interfacial zone[7] as shown in Fig. 3.

The full path-dependent constitutive models were integrated in the scheme of Newmark step-by-step direct integration of both time and strain histories.[9] Figure 3 shows the outline of the proposed material models used for different elements (RC element, RC joint element, soil element and RC/soil interface element), which is hereafter applied in analyzing underground structures.[6]

Definition of underground system

Figure 4a) shows the shape and size of the target's sections. For section A, the RC box culvert has an outer dimension of 17.0 m width and 7.17 m height. The wall thickness is 0.70 m with average reinforcement ratio 0.8%. The thickness of the top and bottom slab are 0.80 and 0.85 m, respectively, with average reinforcement

ratio 1.0%. The intermediate column has a cross-section of 0.40×1.00 m with reinforcement ratio 6.0%. The clear distance between columns in the longitudinal direction is 2.50 m and columns are completely fixed to the top and bottom slabs.

For section B, the outer dimensions are 9.0 m wide and 6.36 m high. The wall and slab thickness are 0.4 m with average reinforcement ratio 1.1%. The cross-section of the column is 0.40×0.60 m with reinforcement ratio 1.6%. The clear distance between columns is 1.90 m. Since the real strength of constituent materials is not known, the authors assumed 24 MPa for compressive strength of concrete and 240 MPa for yield strength of reinforcement.

The model of underground structural system with surrounding soil composed of different layers and all the details of the surrounding soil layers are shown in Fig. 4(c).[1,2] In the analysis, the acceleration wave was applied at the base of layer six because the stiffness of layer seven is large enough to assume this layer as engineering base rock.

The finite element discretization is shown in Fig. 4(d). Since the major direction of the

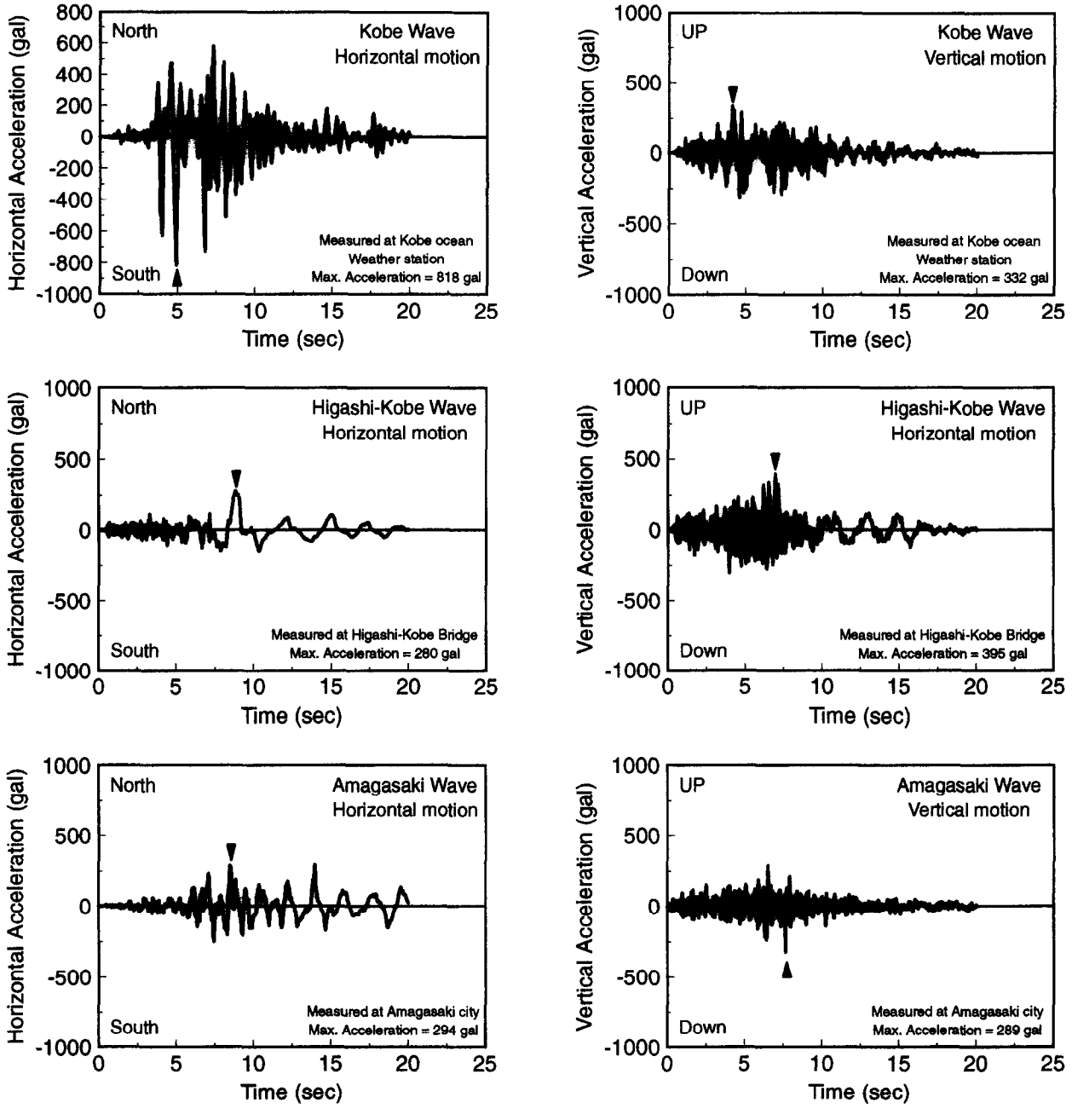

Fig. 2. Acceleration records used in the dynamic analysis.

ground motion was in the transverse direction (north–south) normal to the axis of the subway line, two-dimensional extent of the target was modeled in use of the higher-order isoparametric elements. The mass of total system was considered for computing initial body forces. Mixed artificial boundary model of reflection[11] was put for far field idealization at both extreme sides of soil, as shown in Fig. 4(b, d). The total length of the soil layer is checked to get the minimum appropriate length that can present all the domain and dissipate the energy from finite element analysis domain to far field.

Structural response in time domain

In this section the authors focus on studying the overall response of the structure under the seismic excitation. At the same time, the induced forces to the intermediate column are discussed to identify the failure mechanism.

Structural response acceleration

Figure 5(a) shows the linear response acceleration spectrum (damping coefficient = 3%) for different waves and Fig. 5(b) indicates the nonlinear horizontal response acceleration at the top slab of the RC structure under Kobe wave. Kobe wave evinces the maximum acceleration which arrived so soon after the start of ground motion that the period of vibration is short compared with the other waves.

The maximum nonlinear response acceleration of the finite elements computed is close to 1800 gal in horizontal component, even though the response acceleration spectrum for the 1-DOF linear structural system differs from each other and the maximum acceleration of the linear system (period = 0.1 – 1.0) exceeds 2500 gal. It is because the RC underground structure comes up to the horizontal capacity no matter how different the horizontal response acceleration spectrum of the selected earth-

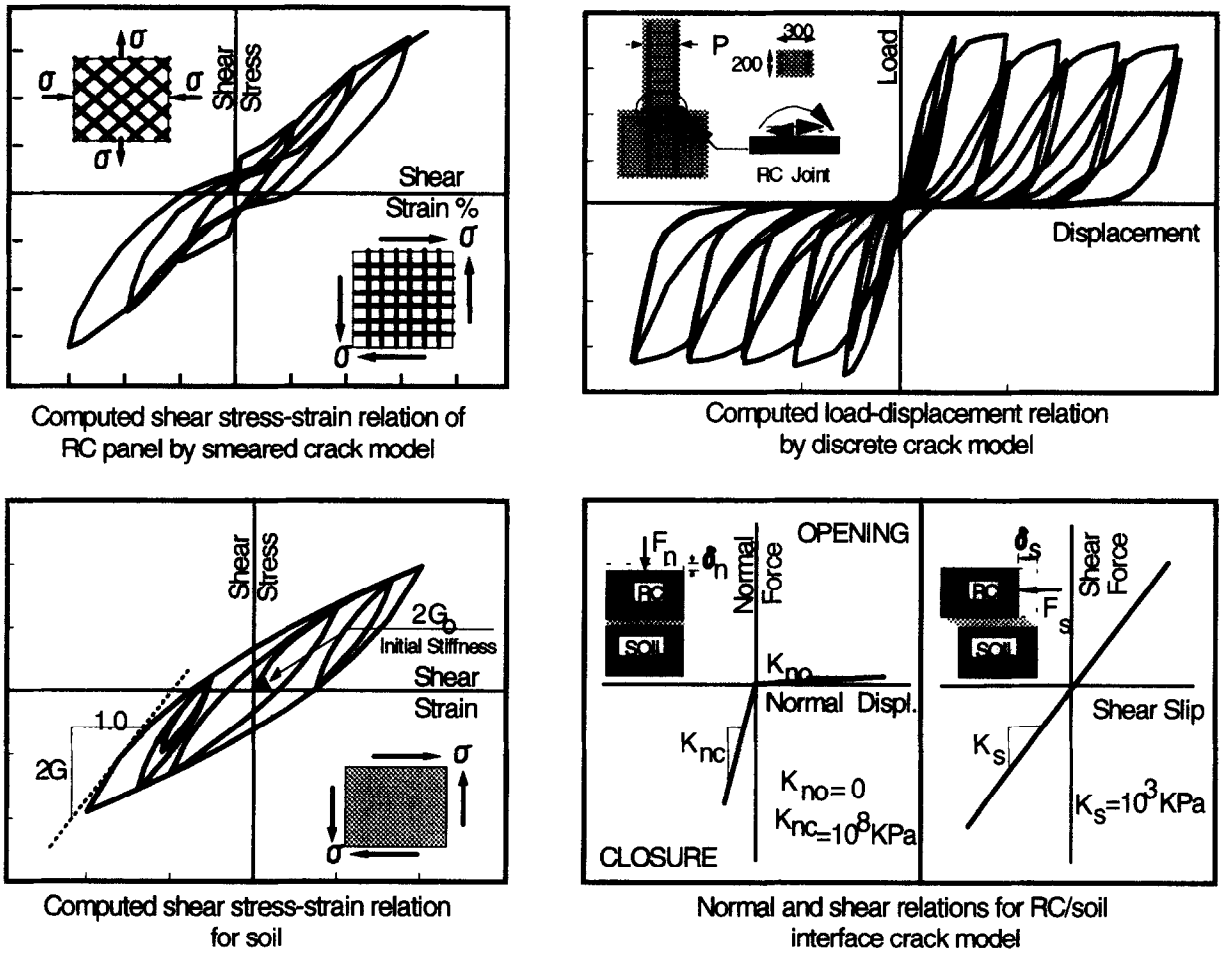

Fig. 3. Outline of constitutive models for different elements.[6]

quake is. Thus, it can be said that the seismic force actually applied to the RC structure would be much beyond the assumed design seismic load and that the recorded earthquake in Kobe was so strong as to exhibit higher response spectrum.

Internal stresses in the intermediate column

Most of damage which affected the underground structures serving the subway in Kobe is concentrated at the intermediate columns. It is important to discuss the induced forces and ductility of the internal columns. Figure 6 shows the internal nominal stresses (compression and shear) and ductility of the column for both sections A and B under different waves.

Figure 6(a) shows the relation between the averaged nominal shear stress and the relative displacement between top and bottom of the column. In these figures, the relative displacement is normalized by the height of the column. For section A under Kobe wave, the column fails with maximum normalized displacement 1.5% and maximum shear stress 16 kgf/cm^2.

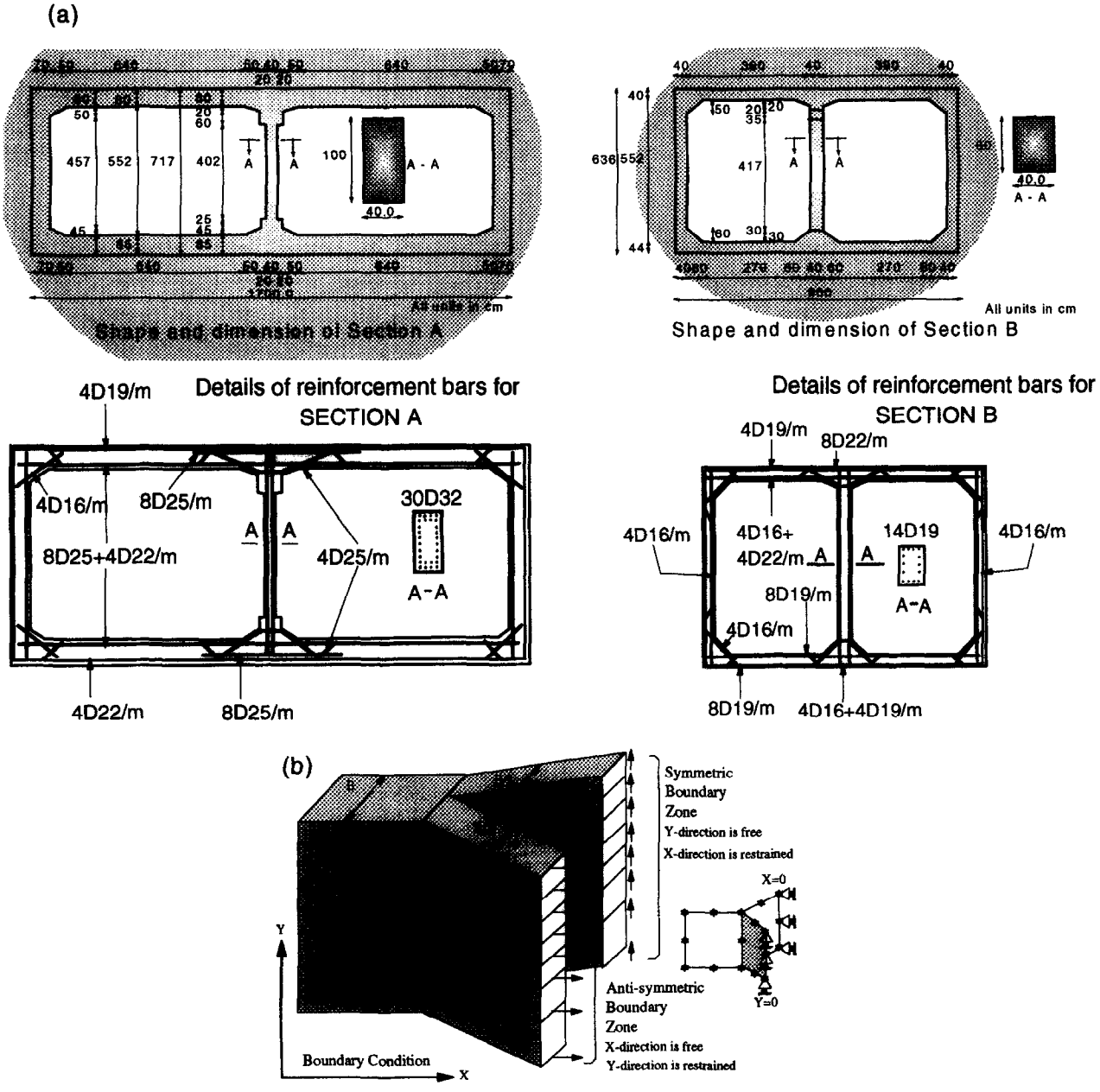

Fig. 4. (a) Shape and dimension of the target structures.[1,2] (b) Overview of the boundary condition.[10].

The yielding of steel takes place before failure. On the other hand, for Amagasaki and Higashi–Kobe waves, the structures survive under the wave with very few cracks.

Although the maximum acceleration of both waves is almost at the same level, the induced shear stress in the case of Amagasaki wave is greater than Higashi–Kobe (about two times).

(c)

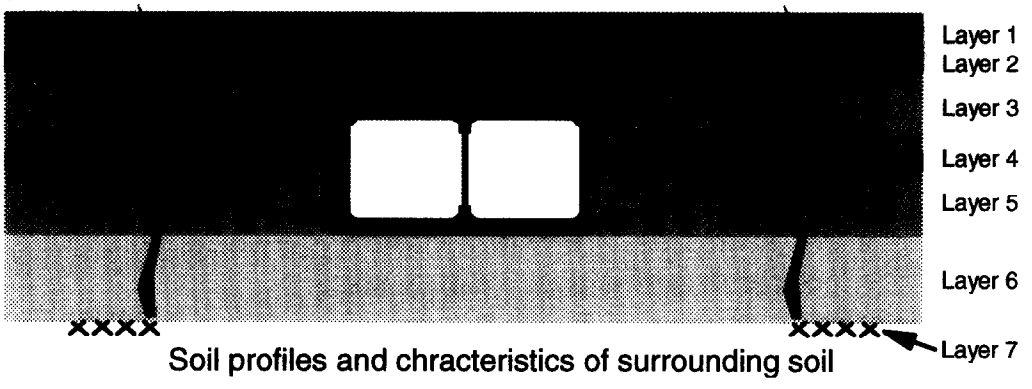

Soil profiles and chracteristics of surrounding soil

	Layer 1	Layer 2	Layer 3	Layer 4	Layer 5	Layer 6	Layer 7
Layer Height (m)	2.20	1.00	5.80	1.10	2.40	4.75	>10.00
SPT-N	8	8	8	9	18	13	90
Vs m/s	188.0	199.0	183.0	197.0	240.0	228.0	453.0
Gs kgf/cm^2	633.0	633.0	633.0	696.0	1212.0	934.0	4391.0
Es kgf/cm^2	1837.0	1837.0	1837.0	2018.0	3514.0	2708.0	12734.0
Weight density t/m^3	1.80	1.60	1.80	1.80	2.10	1.80	2.10
Soil Type	BackFilled	Clay	Sand	Clay	Gravel	Clay	Gravel

(d)

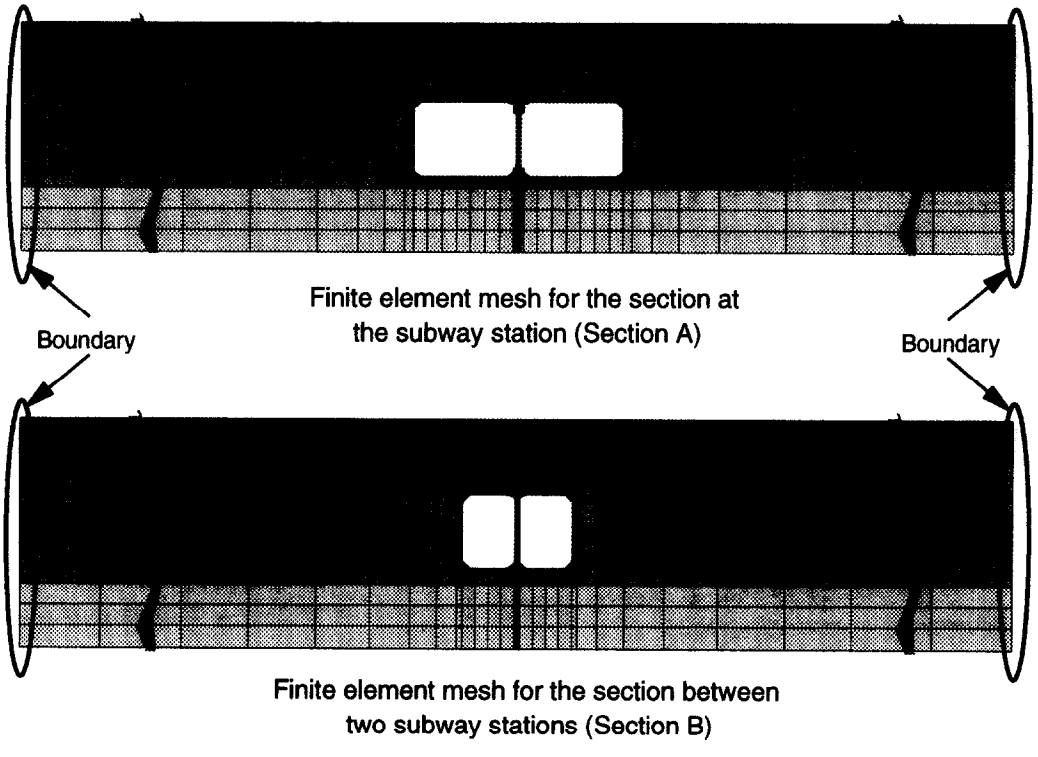

Fig. 1. (c) Soil profiles and characteristics of surrounding soil.[1,2] (d) Finite element discretization used in the analysis.

It can be noted that the induced shear force not only depends on the maximum acceleration, but on the wave phase and its characteristics.

For section B, the structure survives under the Kobe wave with few shear cracks in the column. The maximum normalized displacement is 1.0% with maximum induced shear stress equal to 7.0 kgf/cm^2. For discussing the response of the intermediate column, the variation of nominal compression stress (see Fig. 6(b)) in time domain should be discussed. In the case of section A, the initial compression stress due to static dead loads is equal to 75 kgf/cm^2, but for section B is 38 kgf/cm^2. The variation of compression stress is mainly dependent on the up–down wave. For all cases, the compression stress is increased approximately, until it is 1.8 times the static stress. This value is quite large, due to the comparatively large up–down motion of the ground and this variation affects all response of the column. For evaluating the effect of the up–down motion in more detail, see Section 5.

Inelastic deformation of structure

The spatially averaged inelastic deformation which represents the 'crack strain'[6] associated with yielding of reinforcement crossing cracks, are shown in Fig. 7 in the time domain. The authors use this index to present, qualitatively, how much damage to the structure is induced and how much residual deformation after the earthquake, remains. For section A under the Kobe wave, higher damage and deformation are seen compared with section B. On the other hand, for Amagasaki and Higashi–Kobe, few cracks without any residual deformation occur to the structures.

Failure mode

Figure 8(a) shows the deformational profile of the structure at the failure for section A and for the maximum response for section B. Although the same earthquake wave is used for both sections A and B (Kobe wave), the maximum shear

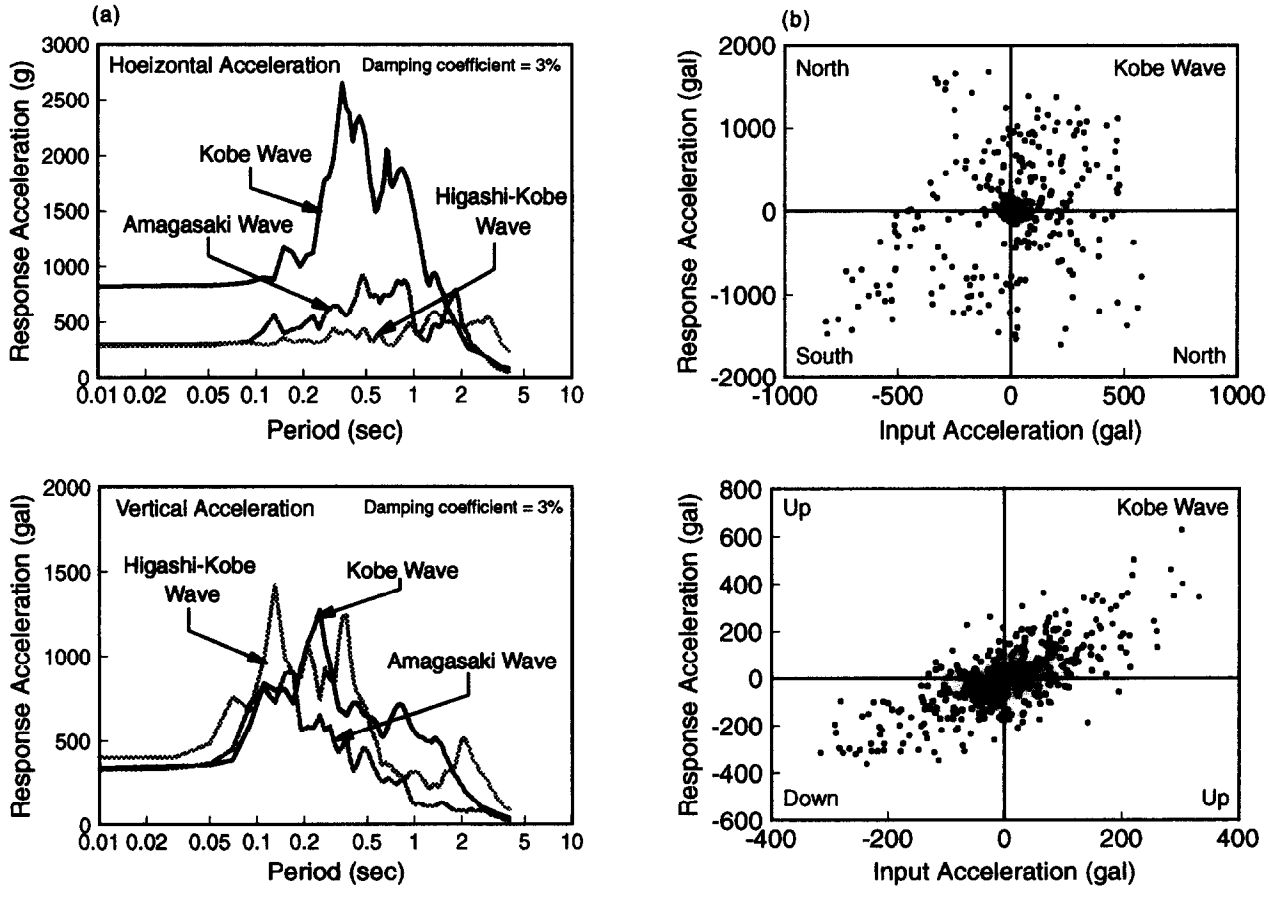

Fig. 5. (a) Response acceleration spectrum. (b) Nonlinear response acceleration diagram.

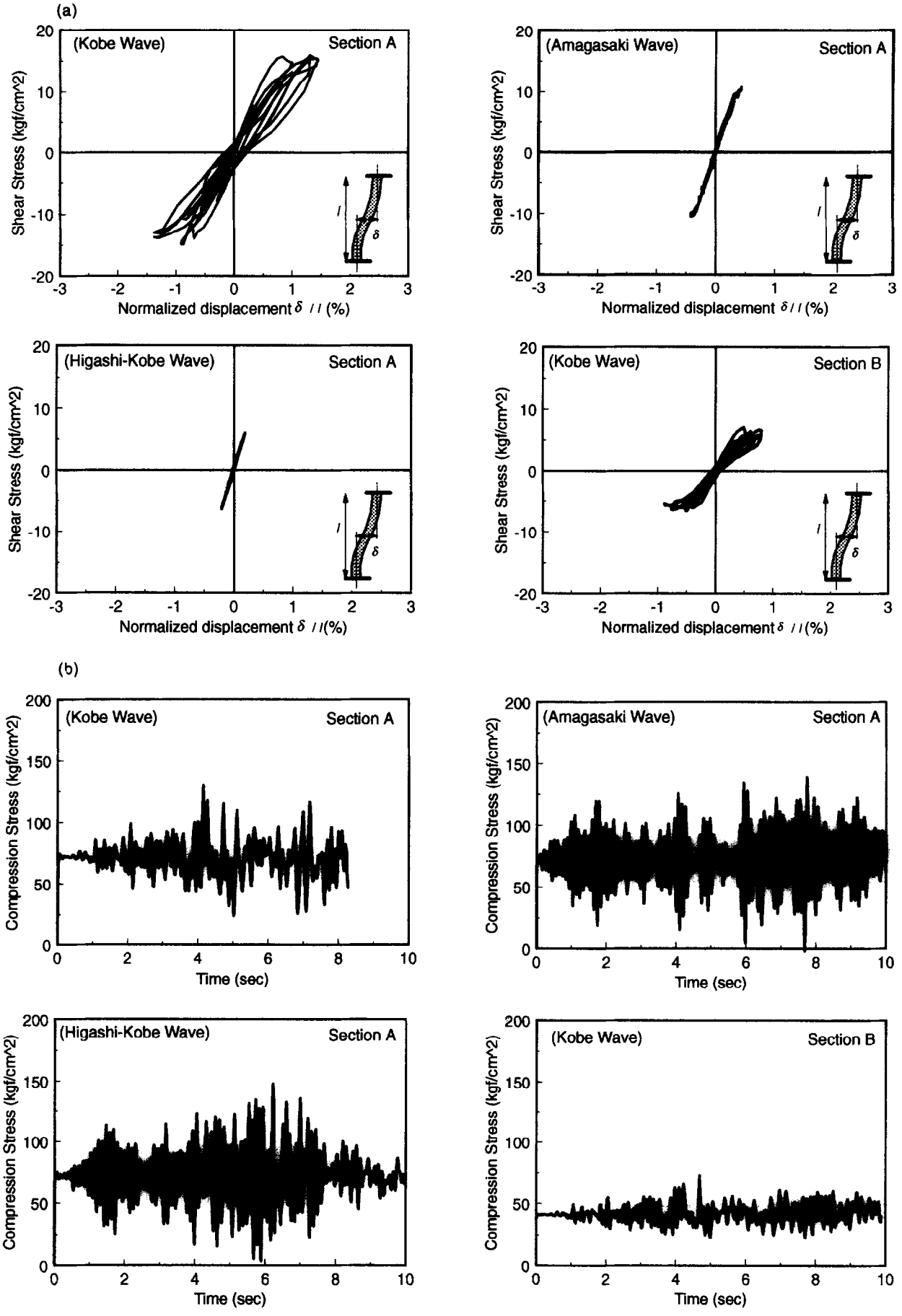

Fig. 6. (a) Shear force–displacement relationship and restoring force characteristics. (b) Variation of compression force in time domain.

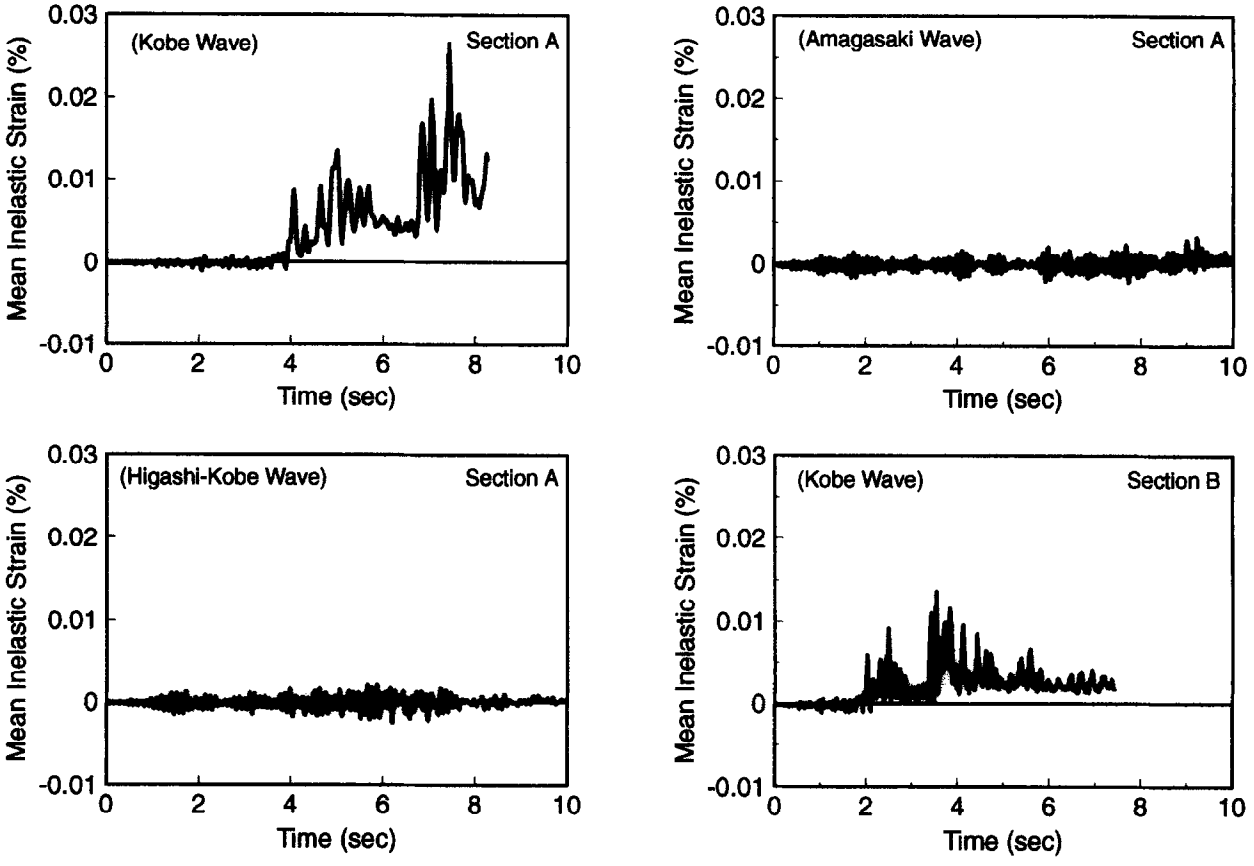

Fig. 7. Inelastic deformation representing damage in time domain.

deformation for section A is greater than section B. It can be seen also that the separation between the soil and RC exists because of the difference between soil and RC shear deformation.

Figure 8(b) shows the crack pattern of the structure at the failure for section A and at the maximum deformation for section B. The cracks having shear strains greater than 0.05% are shown in Fig. 8(b). Other cracks are cut off from the figure for simple illustration.

The computed failure mode of the FE model under the Kobe wave for section A is 'diagonal shear failure' after the yield of main reinforcement in the intermediate column, as shown in Fig. 8(b). Higher shear strain along bi-directional cracks can be seen within the localized zone of the finite elements. At this moment, main reinforcement has already come to the strain hardening at individual cracks.

According to the analyzed failure mode, it is considered that the real RC column would lose axial load carrying mechanism after the creation of the localized diagonal shear band and would finally collapse. Some other cracks exist at the corner of the structure, but with a lower level of strain. For section B, few cracks with small shear strain are shown in Fig. 8(b). These cracks, originated from the flexural action, are distributed in both the column and side walls.

Effect of up–down motion of ground

One of the characteristics of the seismic load in the Kobe area is its higher level of up–down component of the ground motion. For discussing the collapse mechanism, it is worth checking how influential the vertical ground motion was. In general, the vertical component of ground acceleration is ignored in many structural designs, owing to its small contribution to the structural safety and dynamic response. On this line, some trial analysis in which the vertical ground motion was intentionally erased is conducted. In the case of the Kobe wave where the horizontal seismicity is very great, it was computationally found, as shown in Fig. 9(a), that the failure mode and the response are not affected very much by the up–down motion of the ground. The maximum shear stress is not

affected by the vertical motion, but less ductility is obtained by considering the up–down motion. The up–down motion affects the variation of compression stress applied to the column.

However, some difference of the structural responses can be seen in terms of the inelastic deformation when the vertical ground motion is cut off. The spatially averaged inelastic deformation,[8] which represents the 'crack strain', associated with the yielding of reinforcement crossing cracks, is shown in Fig. 9(b) in the time domain. When cut-off of the vertical motion was assumed, induced inelastic strain was reduced with early collapse, compared to the case with which the vertical motion is considered.

It can be concluded that the vertical ground motion is not the primary cause of the collapse of the intermediate column, though some damage caused to the structure could be influenced by the vertical motion of ground. The combination of horizontal and vertical motions changes the internal response of the column which cannot be easily explained through this discussion. For that, more trial analysis under static and dynamic loads are needed for understanding the mechanism of the underground structure under seismic excitation.

COLLAPSE MECHANISM OF INTERMEDIATE COLUMN

Concerning the design of the underground structure, it is important to compare the dynamic response of the structure with the stat-

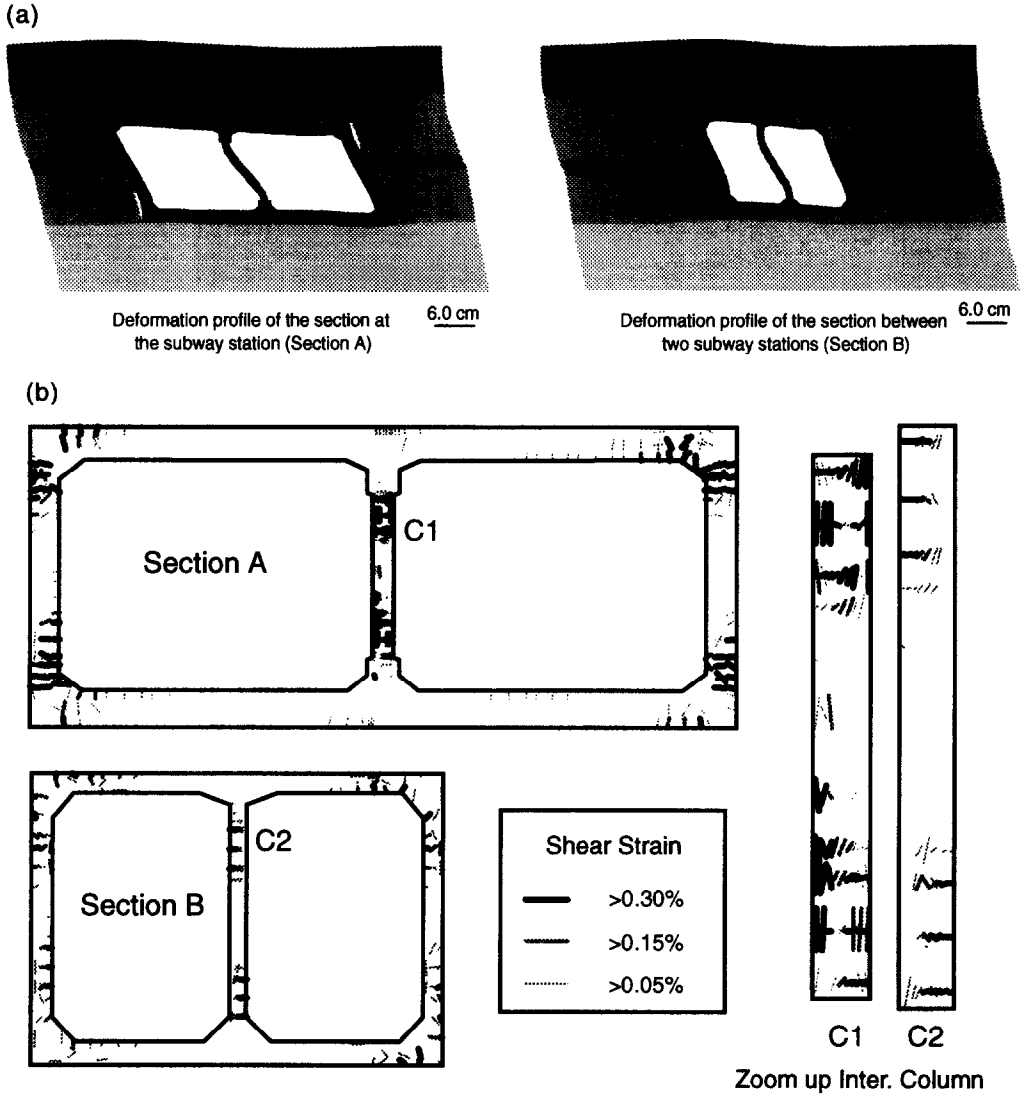

Fig. 8. (a) Deformational profile of the underground structure at the maximum response. (b) Crack pattern of structures at the maximum deformation.

ically obtained capacity and also to determine the maximum ductility of the structure. For that purpose, several static analyses are carried out for different cases, (cases A and B) as shown in Fig. 10. For case A, only the RC column, but for case B, the whole RC structure is analyzed under normal and shear forces. In all cases, the normal compressive force is changed from zero to the maximum capacity of the member. Under the constant compressive force, the shear force is incrementally increased till the failure of the member. By calculating the maximum compression stress, shear stress and maximum displacement from each case, the interaction diagrams can be obtained as shown in Fig. 11.

Figure 11 shows the relation between nominal compressive stress and the ductility of structure, and the relation between the compressive stress and shear stress for both sections A and B. For section A, two lines are the static

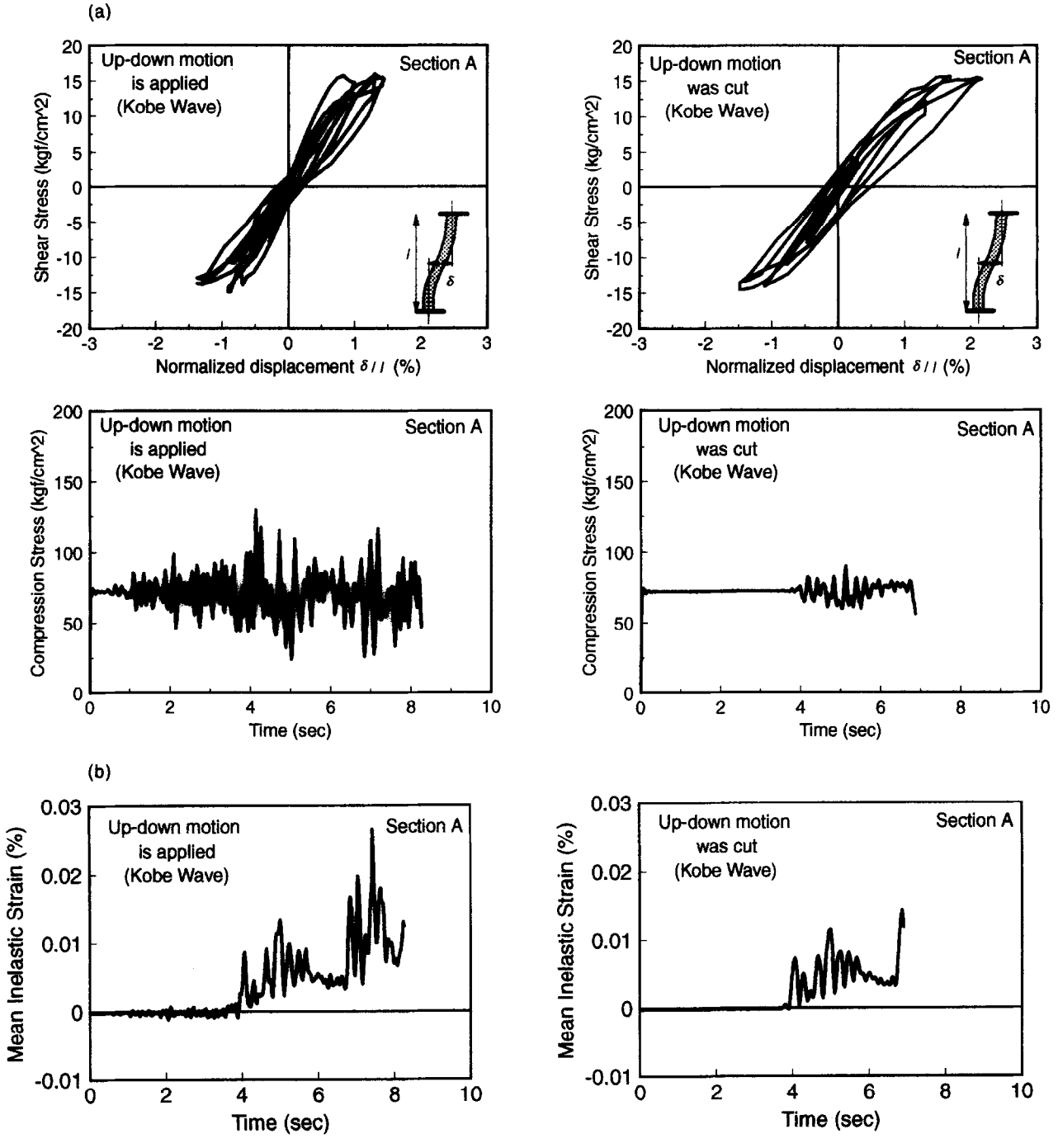

Fig. 9. (a) Effect of vertical component of ground motion in view of internal stresses in the column. (b) Effect of vertical component of ground motion in view of the inelastic deformation of RC.

interaction diagrams of failure for both cases A and B. For section B, only case A can be obtained. For section A, for both cases A and B, the failure of the structure occurred in the intermediate column. For case B, no failure takes place at the intermediate column when we use full model for computing diagram of the intermediate column, because another member failed before the failure of the column concerned.

The dynamic response for sections A and B are shown in Fig. 11. For section B, the maximum dynamic response of structure is located within the failure envelope on the maximum capacity of the member. On the other hand for section A, the dynamic response is closer or higher the static capacity of the member.

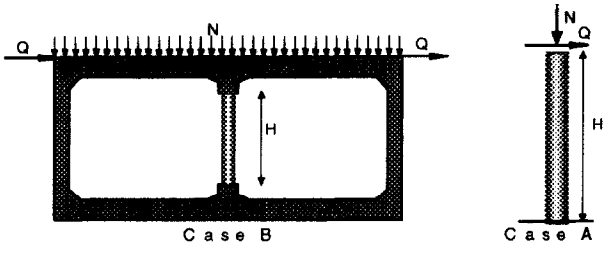

Fig. 10. Details of static load Case A and Case B.

For section A, it is necessary to determine the maximum wave under which the structure can survive. Thus, other dynamic analyses are carried out for the same target (section A) by decreasing the Kobe wave with different ratio. All results are summarized in Fig. 12.

Figure 12 shows the maximum dynamic response for shear, compression stresses and corresponding deformations with respect to the static interaction diagram. It can be concluded that the shear capacity and the ductility of member are not only the parameters which describe the response of the structure, but the compressive capacity is another influencing factor. By increasing the compressive stresses, the ductility is so much decreased. At the same time, the variation of the compression force during the earthquake cannot be ignored, especially in the case of the large up–down motion input.

ENHANCEMENT OF SEISMIC RESISTANCE

Another aim of this study is to discuss the seismic resistant design based on the understanding

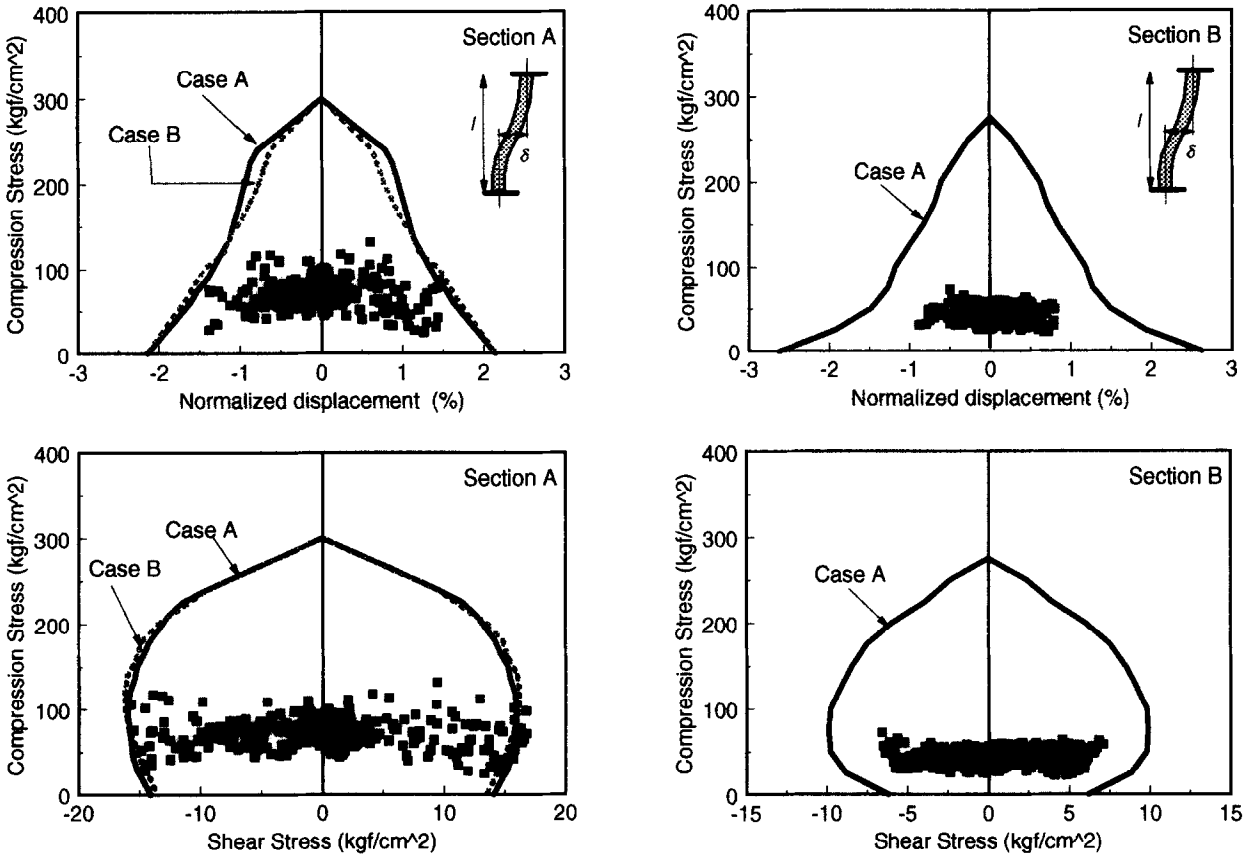

Fig. 11. Failure interaction diagram for maximum response of structure.

of collapse mechanism of the subway station. It has been investigated that most of the damage and collapse of subway station in Kobe city are associated with the shear failure of the intermediate columns. The analyses reported above also indicate the diagonal shear cracks in the nonlinear dynamic simulation. It has also been concluded that the shear capacity and the ductility are the most important parameters which influence the seismic performance. Here, the interaction of these two factors will be discussed for further parametric study.

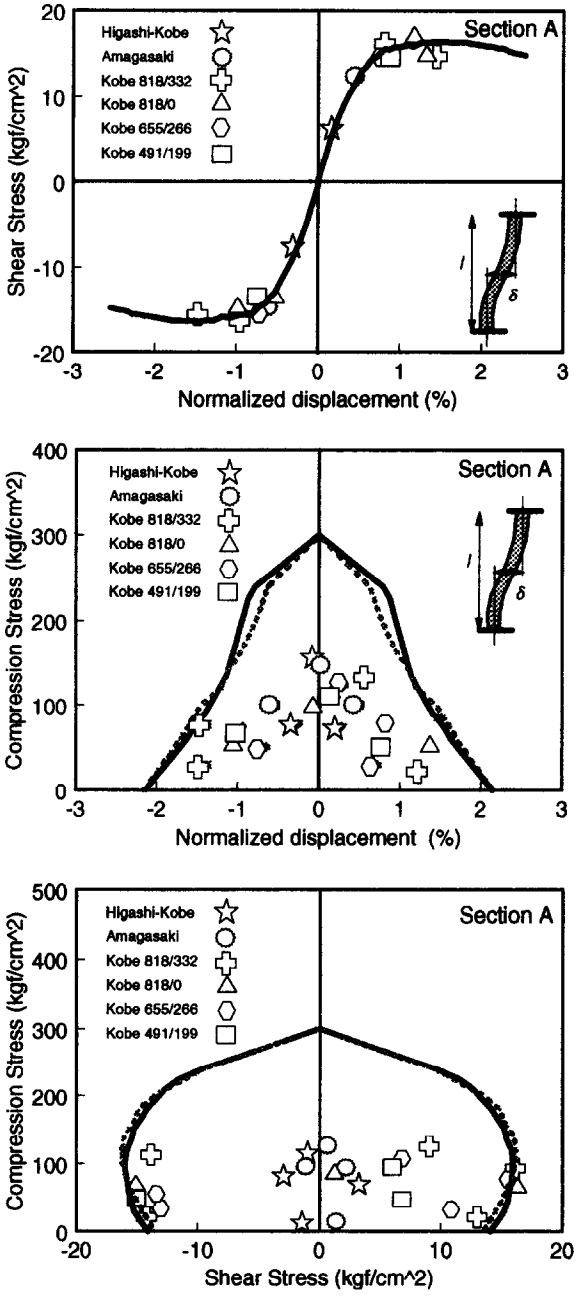

Fig. 12. Interaction diagram for structure response.

For avoiding the shear failure in the RC column, the most simple way is to increase the shear capacity of the column. According to JSCE[12] code, the shear capacity can be described as the following equation.

$$V = V_c + V_s \tag{1}$$

where, V is the shear capacity of the RC member; V_c is the shear force carried by concrete and longitudinal reinforcement; V_s is the shear force carried by the web reinforcement. From eqn 1, for RC member with ordinary concrete strength, there are two ways of increasing the shear capacity. One is to increase the amount of longitudinal reinforcing bars, another is to elevate the web reinforcement. In Fig. 13 it gives two different dynamic responses of the RC column, when using these methods, for increasing the shear capacity.

For the first case, both flexural and shear capacities of this column, defined as M_y and V, will be increased. As the bending capacity is associated with yielding of main reinforcing bars, the yielding shear force, P_y, becomes very large. According to the JSCE code, we have:

$$V \propto (\rho_t)^{\frac{1}{3}} \tag{2}$$

$$P_y = \frac{M_y}{l/2} \propto (\rho_t) \tag{3}$$

where ρ_t is the main reinforcement ratio and l is the height of the column. The yielding shear force increases more than the shear capacity as the amount of main reinforcement rises. RC members with this kind of reinforcement arrangement are very brittle and fail suddenly

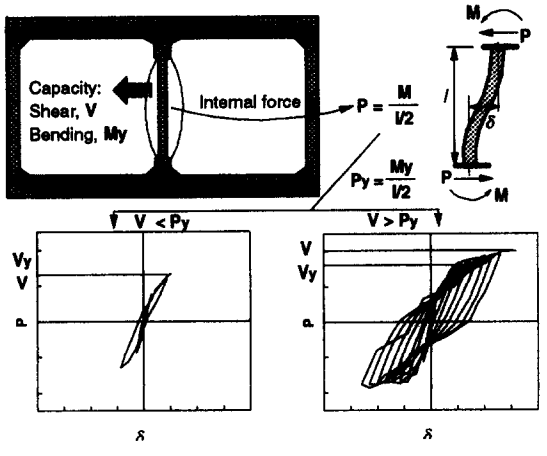

Fig. 13. Interaction of shear capacity and ductility.

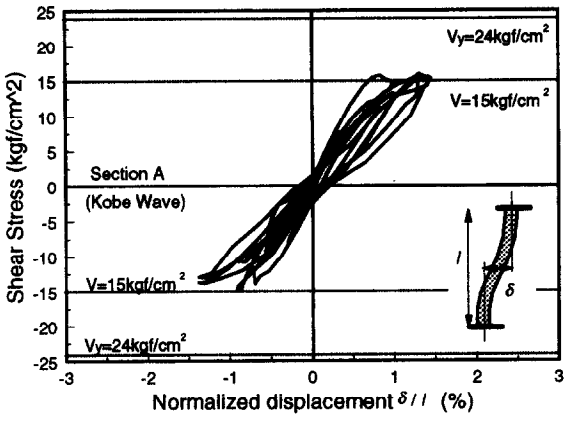

Fig. 14. Brittle shear failure of intermediate column in Daikai station.

without much ductility. The failure of the intermediate columns in Kobe subway stations is categorized into this case (Fig. 14). According to the JSCE code, the shear capacity of the middle column of Daikai subway station is about 15 kgf/cm^2. The experiment for the strength of these columns[13] also proves the shear capacity of 15.3 kgf/cm^2, but the yielding shear strength is 24 kgf/cm^2, that is $V/V_y = 0.64$. During the earthquake the shear stress computed is more than 15 kgf/cm^2. This is why the column failed in shear mode with shear deformation less than 1.5%. On the other hand, if the shear capacity is increased by enhancing the web reinforcement, the shear capacity V can be larger than the yielding shear force V_y. Then the ductility of the RC member will be elevated. RC members having higher shear capacity generally have higher seismic resistant performance.

The above discussion shows the importance of keeping a sufficient amount of web reinforcement to get enough ductility. For this aim, a factor is needed for judging the failure mode as:

$$\frac{V}{V_y} = N \geq N_{req} \tag{4}$$

where, N is a factor which is associated with the failure mode and ductility of RC member. If $N > 1$, the shear failure before the yielding of the main reinforcement can be avoided. In the seismic design of RC structures, the shear failure after the yielding of the main reinforcement should also be avoided for seismic energy absorption. This requires the shear capacity to be larger than the shear force related to the bending capacity of the critical section, which is higher than V_y. For this reason, N_{req} is set larger than 2 for the ductility requirement in seismic design.[14]

EFFECT OF LATERAL TIE REINFORCEMENT AND REDUCTION OF MAIN REINFORCEMENT

In order to enhance the seismic resistance of the subway station, both the shear capacity and the ductility level should be increased. For the existing reinforced concrete structures, one convenient way is to strengthen the columns by increasing the amount of the web reinforcement with steel jacketing. Here the section A of Daikai subway station is used as an example for this study.

According to eqn 4, the ratio of web reinforcement is increased to 1.5% to make the factor N larger than 2. The amounts of main reinforcing bars are kept unchanged. The Kobe wave is used as the input for the dynamic computation. The computation results are shown in Fig. 15.

Figure 15(a) shows the inelastic strain of the subway station during the earthquake. It can be seen that the structure survived without collapse. The maximum damage level is less than 0.02% and is just half of the original case (Fig. 7).

Figure 15(b) shows the shear stress–displacement relationship of the intermediate column. It can be seen that the shear stress comes up to 20 kgf/cm^2. The maximum shear deformation is more than 2%. In comparison with the original case, the shear stress and deformation are larger and the structure can undertake the seismic load. Figure 15(c) shows the compressive stress in the intermediate column. The compressive stress is similar to the original case (Fig. 6(b)).

Another way of enhancing the seismic resistance is to properly reduce the main reinforcement while increasing the amount of web reinforcement. This method is more economical, as fewer reinforcement bars are needed to satisfy eqn 4 and it may be suitable for the design of the new RC structures. The computation based on this kind of reinforcement arrangement is also done for the section A of Daikai subway station under the Kobe wave.

As the compressive stress may exceed 150 kgf/cm^2 in the seismic response, the longitudinal steel bars cannot be reduced so much. In the computation, the main reinforcement is reduced by 10%, compared with the original case where the amount of web is kept as 1.5%, the same as the web enhanced case. The computation as results are shown in Fig. 16.

Figure 16(a) shows the inelastic strain of the subway station during the earthquake. It can be seen that the structure also survived without collapse in the computation. The maximum damage level is around 0.01%, that is small compared to the original case (Fig. 7) and almost half when comparing it to the tie enhanced case (Fig. 15(a)).

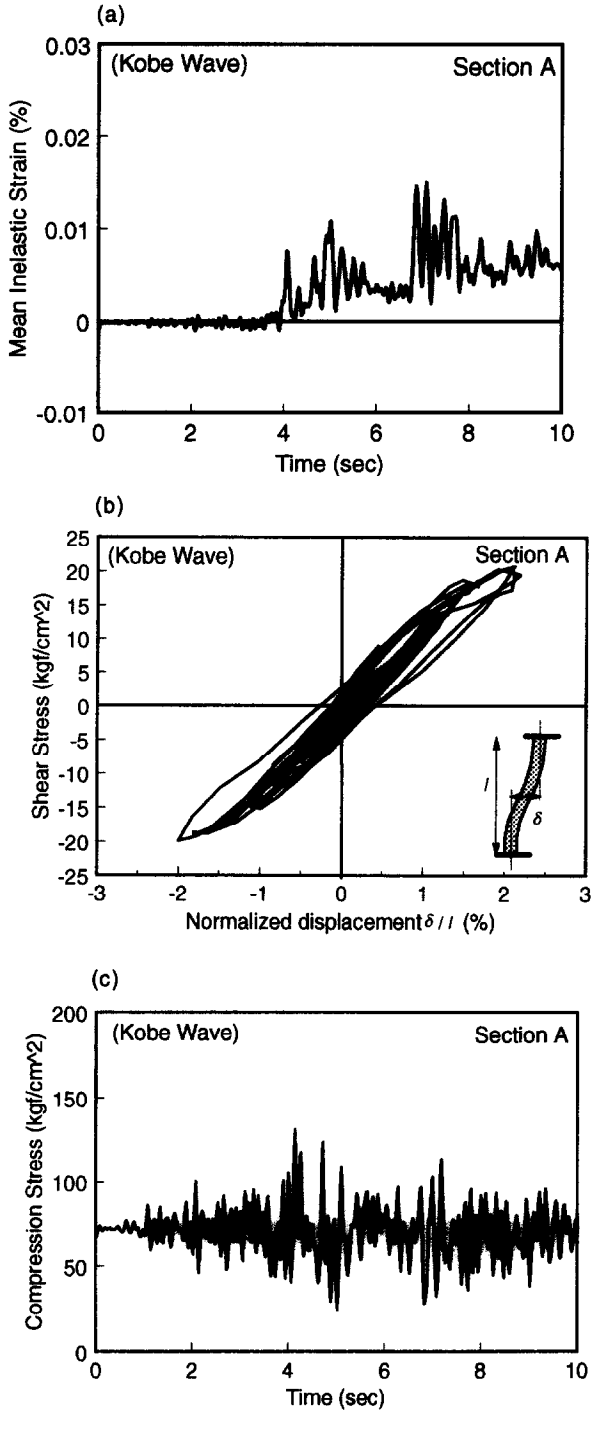

Fig. 15. (a) Inelastic deformation representing damage in time domain. (b) Shear stress-deformation relationship. (c) Variation of compression stress in time domain.

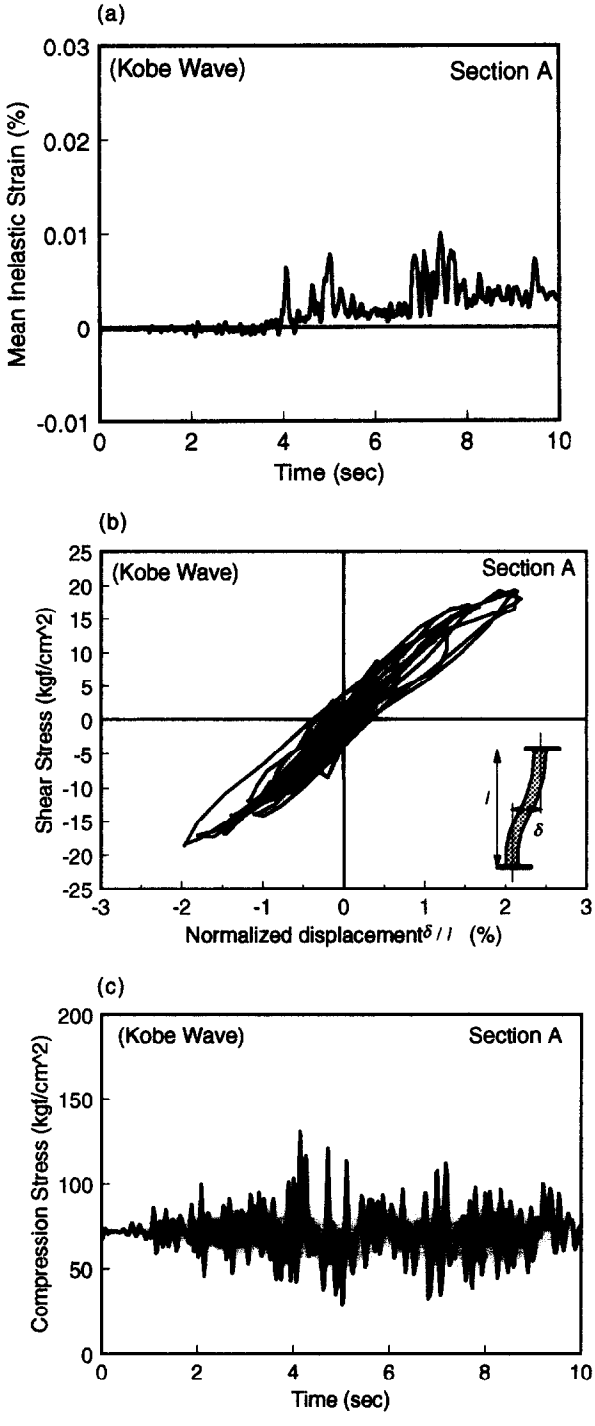

Fig. 16. (a) Inelastic deformation representing damage in time domain. (b) Shear stress-deformation relationship. (c) Variation of compression stress in time domain.

Figure 16(b) shows the shear stress–displacement relationship for the intermediate column. It can be seen that the shear stress reaches 20 kgf/cm^2. The maximum shear deformation is more than 2%. It is almost similar to the enhanced case as the yielding shear stress is still a little higher than the shear stress, so that no obvious yielding takes place at the column. Figure 16(c) shows the compressive stress applied to the intermediate column. It is also similar to the case of web reinforcement enhanced.

These two cases of computation show that the sufficient shear capacity and suitable ductility are two main factors which affect the seismic resistant performance of RC structures. From the parametric study, it can be known that the increasing of web reinforcement is very effective for enhancing the ductility of the RC member. It is shown that if the eqn 4 is satisfied, even though we have less main reinforcement, the structure can survive under heavy earthquakes.

CONCLUSIONS

The collapse mechanism of RC underground structure is still under investigation. Within the authors' analytical discussions based on nonlinear dynamic FEM with path-dependent constitutive laws for cracked reinforced concrete, soil and interface between RC and soil, the following can be tentatively concluded.

The level of seismic excitation actually applied to RC underground structure was beyond the expected design value of the earthquake loads specified when the underground was constructed. The structural ductility and energy absorption are insufficient to survive this great quake, especially the intermediate column which failed in reality.

The comparatively large up–down motion of the ground was measured at several places. The ductility of the structure (intermediate column) is so much decrease by increasing the compression stresses in the column. Compression capacity, shear capacity and ductility are interlinked to determine the safety of underground structure under seismic excitation.

In order to increase the anti-earthquake capacity to shear failure, the shear capacity can be increased by enhancing the web reinforcement. Increasing the main reinforcement is not a suitable way for shear resistance. Keeping a suitable ratio of main and web reinforcement is very important for seismic resistant design.

REFERENCES

1. Yamato, T., Umehara, T. *et al.*, Damage to Daikai subway station, Kobe rapid transit system and estimation of its reason. In *Proceedings of Technical Conference on the Great Hanshin–Awaji Earthquake*. JSCE, Tokyo, 1996, pp. 247–254.
2. Takewaki, N., Ohtsuki, A. *et al.*, An examination on failure mechanism of a subway station due to the 1995 Hyougoken–Nanbu Earthquake. In *Proceedings of Technical Conference on the Great Hanshin–Awaji Earthquake*. JSCE, Tokyo, 1996, pp. 221–226.
3. Shawky, A. & Maekawa, K., Computational approach to path-dependent nonlinear RC/soil. *Journal of Material, Concrete Structures and Pavements, JSCE*, **30** 532 (1996) 197–207.
4. Okamura, H. & Maekawa, K., *Nonlinear Analysis and Constitutive Models of Reinforced Concrete*. Gihodo, Tokyo, 1990.
5. Okamura, H. & Maekawa, K., Reinforced concrete design and size effect in structural nonlinearity, invited. *Proceedings of JCI International Workshop, Size Effect in Concrete Structures*. Sendai, Japan, 1993, pp. 1–20.
6. Shawky, A. & Maekawa, K., Nonlinear response of underground RC structures under shear. *Journal of Material, Concrete Structures and Pavements JSCE*, **31** 538 (1996) 195–206.
7. Shawky, A. & Maekawa, K., Path-dependent computational model for RC/soil system. *Proceedings of JCI*, Yokohama, Vol. 16, No. 2, June 1994, pp. 111–116.
8. Ohsaki, Y., Some notes on Masing's law and nonlinear response of soil deposits. *Journal of Faculty of Engineering, University of Tokyo*, **35** 4 (1980) 73–158.
9. Song, C. & Maekawa, K., Dynamic nonlinear finite element analysis of reinforced concrete. *Journal of Faculty of Engineering, University of Tokyo*, **12** 1 (1991) 384–407.
10. Shawky, A. & Maekawa, K., Nonlinear dynamic analysis for underground reinforced concrete structures. *East Asian–Pacific Conference on Structural Engineering and Construction*, EASEC-5, Australia, July 1995.
11. Shawky, A. & Maekawa, K., Dynamic nonlinear interaction of underground RC/soil system. *Proceedings of the First Cairo Earthquake Symposium on Seismic Risk Assessment*, December 1994.
12. JSCE, Standard specification for design and construction of concrete structure, Part I (Design), 1st edn. Tokyo, 1986.
13. Iida, H., Aoki, H. *et al.*, The strength and ductility of restored and suffered center pillar at Daikai subway station based the experiment. *Proceedings of Technical Conference on the Great Hanshin–Awaji Earthquake*. JSCE, Tokyo, 1996.
14. JSCE, Standard specification for seismic resistant design of concrete structure, Tokyo, 1996.